ELSEVIER

Atmospheric Environment 38 (2004) 2951–2964

ATMOSPHERIC ENVIRONMENT

www.elsevier.com/locate/atmosenv

The nature of individual solid particles retained in size-resolved raindrops fallen in Asian dust storm event during ACE-Asia

Chang-Jin Ma[a,*], Susumu Tohno[a], Mikio Kasahara[a], Shinjiro Hayakawa[b]

[a] *Department of Socio-Environmental Energy Science, Graduate School of Energy Science, Kyoto University, Uji, Kyoto 611-0011, Japan*
[b] *Graduate School of Engineering, Hiroshima University, Higashi-Hiroshima, Hiroshima 739-8527, Japan*

Received 5 June 2003; accepted 5 March 2004

Abstract

To determine the physicochemical properties of individual solid particles retained in raindrops, the size-segregated raindrop sampling was carried out at ground-based site in Kyoto, Japan in Asian dust storm event during ACE-Asia. For the analysis of elemental components in individual solid particles, X-ray fluorescence microprobe system installed at Super Photon ring 8 GeV (SPring-8) BL-37XU was applied. Consequently interraindrop data of individual solid particles that are present inside the raindrops could be obtained. The number size distribution of individual solid particles scavenged by each raindrop size was compared to the calculated particle-scavenging coefficient (E). There was a good agreement between the calculated scavenging coefficient for particles and the measured number size distribution of particles with radius 1 μm. Elemental mass showing the peak at raindrops collected on 0.7 mm mesh size was varied as a function of raindrop size. The masses of crustal components and chlorine show significantly high level regardless of raindrop size. Individual residual particles were successfully classified into several factors as a function of raindrop size. The hygroscopic portions for S, Cl, K, and Ca in individual particles retained in size-segregated raindrop were determined. The mixed particles with crustal and sea-salt accounted for large fraction of particles retained in small raindrops. Whereas, in the case of large raindrops, the mixed residual particles with crustal and sulfur contributed to large portion. The results obtained from our study indicate that a large number of dust particles were incorporated into cloud droplets during their long-range transport and dust particles were effectively washed out by raindrops during rainfall event.

Keywords: Asian dust storm; ACE-Asia; Size-resolved raindrop; Residual particle; Scavenge; Wet deposition

1. Introduction

In China, owing to the development of agriculture, the area of land adversely affected by sand has gradually increased, and during the 1950s and 1960s the land affected by sand expanded at an average of 1600 km^2 per year. By the 1990s, the area by which this land was expanding had reached 2500 km^2 per year. Wind blown dust originating from the arid deserts of Mongolia and China is a well-known springtime meteorological phenomenon throughout East Asia. In fact, this Asian dust storm phenomenon is called "Huangsha", "Whangsa", and "Kosa" in China, Korea, and Japan, respectively. This dust is blown up by strong wind behind the cyclone and delivered in free troposphere by westerly jet. Even though Asian dust storm is a peculiar phenomenon occurring in China continent, this Asian dust storm has led to a significant environmental change in East Asia and North Pacific Ocean for a long time. A large number of studies on the Asian dust storm aerosols

*Corresponding author. Tel.: +81-774-38-4413; fax: +81-774-38-4411.
E-mail address: ma@uji.energy.kyoto-u.ac.jp (C.-J. Ma).

1352-2310/$ - see front matter © 2004 Elsevier Ltd. All rights reserved.
doi:10.1016/j.atmosenv.2004.03.025

have been reported (Duce et al., 1980; Darzi and Winchester, 1982; Braaten and Cahill, 1986; Iwasaka et al., 1988; Ma et al., 2001a).

This dust finally dissipates when the particles are removed from the atmosphere by dry and wet removal processes. Gravitational settling of large particles ($>10\,\mu m$) occurs near the source within the first day of transport. Wet removal occurs sporadically throughout the 5–10 days lifetime of the remaining smaller size dust particles. If the relative humidity of the air parcel reaches a critical humidity, the value of which depends on the size and chemical composition of the aerosol present, the droplets become activated, grow freely by water vapor diffusion, and cloud droplets are formed. This in-cloud scavenging of particles is called rainout. Whereas, washout occurs below-cloud during raining. This washout process comprises Brownian diffusion, interception, and impaction (Pilat and Prem, 1976; Seinfeld, 1986). And those washout processes have been simulated in many publications (Pilat and Prem, 1976; Flossmann et al., 1985; Chate and Kamra, 1997; Chen, 2002). The major mechanism of the incorporation of particulate matter into raindrops is the collision among the particles below the cloud base. The efficiency of the collision depends on the size distributions of particles and the raindrops (Flossmann et al., 1985; Nicholson et al., 1991; Mcgann et al., 1993; Byrne and Jennings, 1993). Large particles are scavenged from the atmosphere more rapidly than small ones. This implies a greater efficiency of scavenging sea-salt and mechanically generated alkaline dust compared with particles of anthropogenic origin (Lei and Tanner, 1997). This mechanism increases the pH of the rainwater, because alkaline ions such as Na^+ and Ca^{2+} are more abundant among large particles.

Because the chemical content of raindrops is variable according to the multiple complex scavenging mechanisms, the chemical processes in the atmosphere such as the washout of particles and gases are not sufficiently described by the usual determination of elemental concentration in rainwater (Tenberken and Bächmann, 1996; Ma et al., 2001b). Therefore the sampling and analysis of individual raindrops must be performed (Tenberken and Bächmann, 1996; Ma, 2001). Tenberken and Bächmann (1996) introduced the "Guttalgor" method that can collect individual raindrops and size-classified raindrops. Furthermore they applied the capillary zone electrophoresis method to the analysis of individual raindrops.

As mentioned above, many researches about atmospheric Asian dust storm particles have been reported. However, no study on the individual Asian dust storm particles scavenged in size-segregated raindrops, which can provide detailed information about the removal characteristics of Asian dust storm particles, was reported.

In the present study, to estimate the physiochemical properties of individual solid particles retained in raindrops, we collected the size-classified raindrops at ground-based site during Asian dust storm event and analyzed the elemental components in particles that are present inside the raindrops using X-ray fluorescence (XRF) microprobe system. Moreover, the physical properties of particles scavenged by raindrops were compared to the calculated particle-scavenging coefficient of size-resolved raindrops.

2. Experimental

2.1. Sampling site

Size-segregated raindrop sampling was conducted on a five-story building of Kyoto University located in Kyoto (34.53°N; 135.48°E), Japan during rain events in the early of April 2001. A filled circle in Fig. 1 indicates the location of sampling site. Kyoto Prefecture, located in the middle of the Main Island of Japan, forms a long shape, extending from the northern coast on the Wakasa Bay through the Kyoto Basin up to the southern region bordering on Mie Prefectures. The prefecture has a total land area of $4612\,km^2$ and a total population of about 2.6 million (ranked 13th nationally). The climate of Kyoto is much affected by the geographical features of the prefecture—its length from north to south, and its topographical variety of the Tango Mountains, the Tanba Plateau, and the Kyoto Basin. The average annual temperature of Kyoto Prefecture is 15.3°C.

2.2. Sampling and handling

To collect the size-classified raindrops, "Guttalgor method" presented by Tenberken and Bächmann (1996) was modified in this study. The sampling apparatus consists of a dewar vacuum flask filled with liquid nitrogen and five-stage stainless steel sieves (Nonaka Rikaki Co.). Fallen raindrops in the liquid nitrogen are frozen and they sink to lower sieves owing to their higher density. The raindrops kept their spherical shape during the freezing process. Consequently, by using stainless steel sieves of different five-step mesh pore sizes (back-up, 0.5, 0.7, 1.0, 1.7 mm), it was possible to separate the frozen raindrops according to their size. Raindrops were collected for about 5 min in the beginning of rainfall considering the rainfall intensity. For the handling of single raindrops without evaporation and contamination, we used a clean air chamber system designed by Ma (2001). After sampling, the sieves were pulled out from the dewar vacuum flask and the frozen raindrops on each sieve were placed into the polyethylene vial by using vacuum pipette (Hako 392). Every handling process was performed in clean air

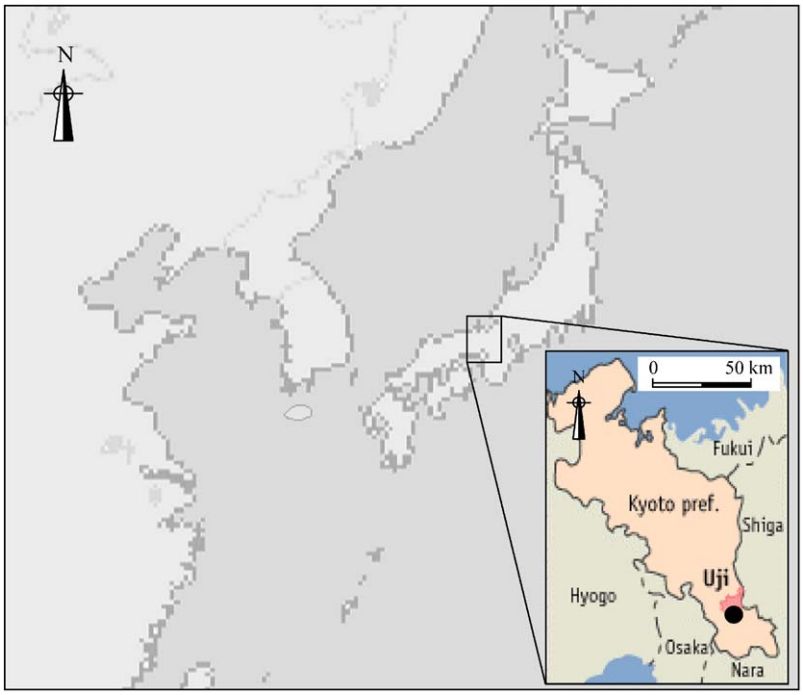

Fig. 1. Location of the size-segregated raindrop sampling site indicated by filled circle.

system filled with the cool nitrogen gas. More details about sampling and handling processes of raindrops are described elsewhere (Ma, 2001). To separate the solid particles from frozen raindrops, the frozen raindrops were melted and centrifuged under the condition of 4000 rpm (maximum centrifugal force: 2670*g*) for 10 min. And then the solid particles were deposited on 10 μm thickness Mylar film. Subsequently they were analyzed.

Moreover, concurrently with the frozen raindrop sampling, the residues scavenged and incorporated into raindrop were arrested using the collodion film replication technique introduced by Ma et al. (2003). This replication technique for individual raindrops enables us not only to keep a whole raindrop on the film surface, but also to analyze residual materials The raindrop replication method was similar to those described elsewhere (Ma, 2001; Ma et al., 2003) and was noted here briefly. Collodion solution was made by dissolving the nitrocellulose involving 11–12% of nitrogen into ethyl alcohol. 200 μl of collodion solution was mounted onto the 10 μm thickness Mylar film just before sampling. Freely falling raindrops were allowed to settle on the surface of collodion film (130 ± 10 μm) without bouncing off.

2.3. Chemical analysis

For the quantification analysis of the ultra trace elements in the individual solid particles retained in raindrops, the XRF microbeam system equipped at Super Photon ring 8 GeV (SPring-8) BL-37XU was applied. Hayakawa (2000) has developed this BL-37XU at SPring-8 that chemically analyzes the various specimens. This method has been successfully used to carry out the reconstruction of elemental map and the quantification analysis for multiple elements with ~femto gram level sensitivity (Hayakawa, 2000; Hayakawa et al., 2001). The experimental setup for XRF microprobe is schematically illustrated in Fig. 2. To make narrow the X-ray beam with micro scale, a pair of elliptical mirrors (Kirkpatrick and Baez mirror, KB mirror) was installed to the optical path. A combination of the focusing mirror and a fixed exit monochromator has enabled energy tunable X-ray microbeam. The samples were placed on the XY stage in a vacuum chamber, and the takeoff angle of 10° was used for the measurement. The intensity of the incident X-rays was monitored by an ionization chamber. The fluorescent X-rays were recorded with a Si (Li) detector placed in the electron orbit plane of the storage ring and mounted at 90° to the incident X-rays to minimize the background caused by the scattering. To avoid excessive counting rate, the sample–detector distance of 100 mm was used. The more detailed analytical procedures and experimental setup used for XRF microprobe analysis can be found in Hayakawa et al. (2001).

Furthermore, in order to obtain the information on raindrop residues, micro-Particle Induced X-ray

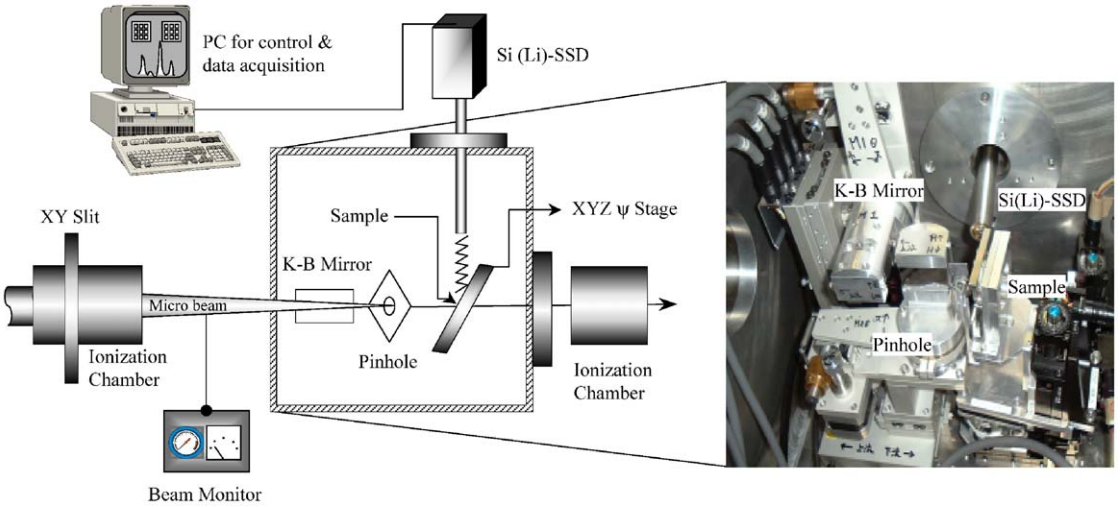

Fig. 2. Schematic illustration of the experimental setup for XRF microprobe at SPring-8, BL37XU.

Emission (PIXE) analysis was employed. Micro-PIXE analysis was performed with a scanning 2.5 MeV H^+ micro beam accelerated by 3 MV single-end accelerator. Beam diameter and beam current were 1–2 μm and >100 pA, respectively. More details about the micro-PIXE analytical procedures and experimental setups can be found elsewhere (Ishii et al., 1996; Ma et al., 2003).

3. Results and discussion

3.1. Physical properties

Fig. 3 presents the number size distribution of solid particles scavenged by each raindrop size. To calculate the number size distribution, we measured indiscriminately the size of 200 individual particles for each five-step raindrop size by microscopic (Keyence, VH-7000) observation. However, unfortunately particles smaller than 0.5 μm diameter were not included because of the resolution ability of microscope. As shown in Fig. 3, the main peak was formed around 1 μm diameter particle size. Also the small miner peak was shown between 3 and 4 μm particle size. In general, in the atmosphere, there is a tendency towards higher number concentration in the smaller particle. The size-classified airborne particle number concentration was observed in Seoul during Asian dust storm period in spring 1998 by Chun et al. (2001). In their study, the particle number concentrations for different three Asian dust storms showed the sharp increase with decreasing particle size. However, in the present study, the strong decrease of the particle number concentration between 1 and 0.5 μm was observed. As one of the possible reasons for this result, the anthropogenic aged particles such as sulfate, nitrate, and ammonium formed by gas-to-particle conversion accounting for fine particles are completely dissociated as ionic state in raindrop. Also, according to the hygroscopic portion of Asian dust storm particle, it can be thought that left shifting of number size distribution line for coarse particles was occurred. Seinfeld and Pandis (1998) reported that the soluble species that exist below cloud were dissolved into falling raindrops during rainfall. Elsewhere, from Fig. 3 we can indirectly discuss the characteristics of particle scavenging by raindrops as a function of their size. Due to the water-soluble fraction of particles, the actual property of particle scavenging will not be directly compared to the laboratory measurements of the scavenging efficiency. However, different shapes of number size distributions curves are found as a function of raindrop size. Particles with radius around 0.5 μm show the maximum number size distribution at $Rd_{0.5mm}$. On the other hand, the number size distribution for particles with radius 1 μm was decreased with increasing raindrop size except $Rd_{0.5mm}$.

When a raindrop falls through air, the below-cloud-scavenging rate of aerosol particles with radius (r_p) in the volume of a cylinder can be written as

$$\frac{d\delta m(r_p)}{dt} = -\Lambda(r_p)\delta m(r_p), \quad (1)$$

where δm is the mass distribution of aerosol particle, and r_p is the radius of aerosol particles. As mentioned earlier, in the atmosphere, aerosol particles can be mainly removed through the processes of Brownian diffusion, interception, and impaction. Also other mechanisms like diffusiophoresis, electrostatic force, and thermophoresis are comprised in particle scavenging by raindrop. In this study, to estimate the particle

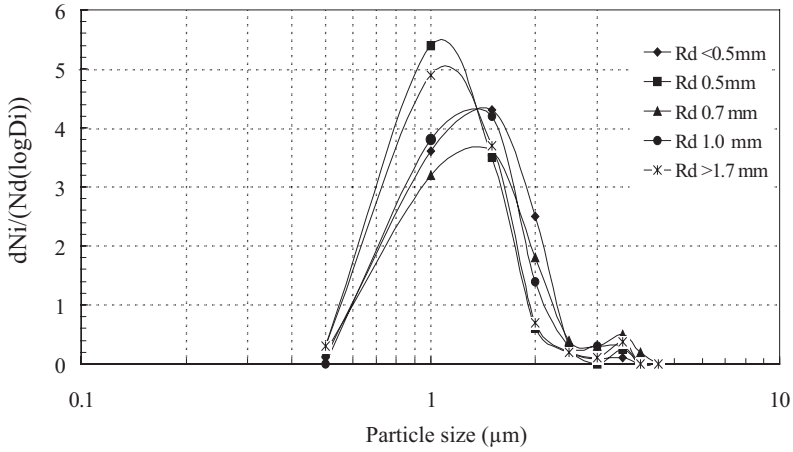

Fig. 3. Number size distribution of particles scavenged by size-segregated raindrops. Particles smaller than 0.5 μm are not included because of the resolution ability of microscope.

collection efficiency (E) of raindrops including Brownian diffusion (E_{dif}), interception (E_{int}), inertial impaction processes (E_{imp}), and combined with these three, particle-scavenging coefficient (E_{com}) of size-resolved raindrops was calculated. Because Brownian diffusion, random motion of the particles, decreases rapidly as particle size increases, one can expect that this removal mechanism will be most important for the smaller size particles with diameter $<0.2\,\mu m$. Interception takes place when a particle, following the streamlines of flow around an obstacle, comes into contact with the raindrop, because of its size. Inertial impaction increases in importance as the aerosol size increases and accelerates scavenging of particles with diameters $>1\,\mu m$ (Seinfeld and Pandis, 1998). In order to formulate a correlation for E based on dimensional analysis, the parameters that influence E must be identified (Seinfeld and Pandis, 1998). The parameters are several variables such as volume of raindrop (f, cm^3), scale height (H, m), rain intensity (I, $mm\,h^{-1}$), total number concentration of raindrop (N, m^{-3}), raindrop radius (r_r, μm), Reynolds number (Re), critical Stokes number (S^*), raindrop terminal settling velocity (U_t, $cm\,s^{-1}$), rainwater concentration in the atmosphere (W, $mg\,m^{-3}$), vertical distance from the cloud base (z, m), scavenging coefficient (Λ, s^{-1}), dynamic viscosity of air (μ_a, Pa s), particle diffusivity (D_p, $cm\,s^{-2}$) and dynamic viscosity of water (μ_r, Pa s). Based on E_{dif}, E_{int}, and E_{imp}, Strauss (1975) proposed the following E_{com} equation that fits experimental data:

$$E_{com} = 1 - (1 - E_{dif})(1 - E_{int})(1 - E_{imp}), \quad (2)$$

where E_{dif}, E_{int}, and E_{imp} are the particle collection efficiencies of raindrops by Brownian diffusion, interception, and inertial impaction, respectively. In the present study, the following E_{dif}, E_{int}, and E_{imp} proposed by Slinn (1984) were applied.

$$E_{dif} = \frac{4}{Re\,Sc}(1 + 0.4\,Re^{1/2}Sc^{1/3}), \quad (3)$$

$$E_{int} = 4\frac{r_p}{r_r}\left(\frac{\mu_a}{\mu_r} + (1 + 2\,Re^{1/2})\frac{r_p}{r_r}\right), \quad (4)$$

$$E_{imp} = \left(\frac{St - S^*}{St - S^* + 2/3}\right)^{3/2}, \quad (5)$$

where Re is the Reynolds number of raindrop based on its radius ($(r_r U_t \rho_a)/\mu_a$), Sc is the Schmidt number of collected particle ($\mu_a/\rho_a D_p$), St is the Stokes number of collected particle ($(2C\rho_p r_p U_t)/(9\mu_a r_r)$), C is the Cunningham slip factor, ρ_p is the particle density ($kg\,m^{-3}$), and $S*$ is the Critical stokes number ($((1.2 + (1/12)\ln(1 + Re))/(1 + \ln(1 + Re))$).

Therefore the scavenging coefficient $\Lambda(r_p, s^{-1})$ is given by

$$\Lambda(r_p) = \int_0^\infty r_r^2 E_{com}(r_p, r_r) N(r_r) U_t(r_r)\,d(r_r), \quad (6)$$

where r_r is the radius of raindrop. $N(r_r)$ is the size distribution of raindrops.

For the size distribution of raindrops, $N(r_r)$, the following equation proposed by Mashall and Palmer (1948) was applied:

$$dN(r_r)/dr_r = 0.08\exp(-41 r_r I^{-0.21}). \quad (7)$$

The terminal velocity of raindrops (U_t, $cm\,s^{-1}$) was applied by the Beard's (1976) three physically distinct flow regimes: (1) small cloud droplets, $1\,\mu m \leqslant d_0 \leqslant 20\,\mu m$ (steady wake, vanishingly small Reynolds number, $10^{-6} \leqslant N_{Re} \leqslant 0.01$), (2) large cloud droplets to small raindrops, $20\,\mu m \leqslant d_0 \leqslant 1\,mm$ (steady wake, low to intermediate Reynolds number, $0.01 \leqslant N_{Re} \leqslant 300$), (3) small to large raindrops, $1\,mm \leqslant d_0 \leqslant 7\,mm$ (unsteady

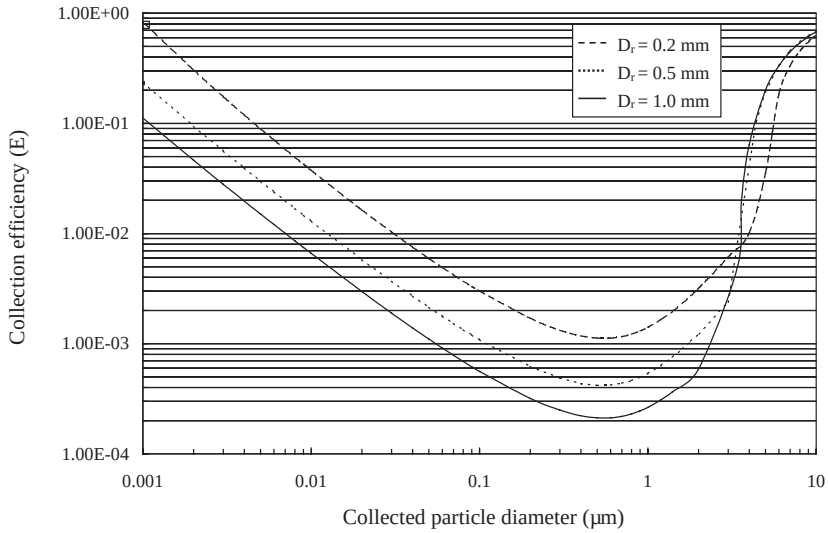

Fig. 4. Particle scavenging coefficient as a function of raindrop size for combined with Brownian diffusion, interception, and inertial impaction. D_r is raindrop diameter.

wake, moderate to large Reynolds number, $300 \leqslant N_{Re} \leqslant 4000$). Fig. 4 shows the scavenging coefficient for monodisperse particles as a function of their diameter collected by monodisperse raindrops with diameters 0.2, 0.5, and 1 mm. This figure indicates the sensitivity of the scavenging coefficient to sizes of both particles and the raindrops as well as suggests the need for realistic size distributions for both particle and raindrops in order to obtain useful estimate for ambient scavenging rates. The relative increase of the E with decreasing raindrop size was shown. Also there is a continuous decrease in E with increasing particle size smaller than 0.5 μm diameter. E has a minimum in the 0.4–0.6 μm particle diameter range. This minimum range can be referred as the "Greenfield gap" suggested by Greenfield (1957) and is due to Brownian diffusion domination particle capture for particle radius <0.05 μm and due to impaction domination particle capture for particle radius >2 μm. Subsequent investigators such as Slinn and Hales (1971), and Pilat and Prem (1976) included the phoretic processes of thermophoresis and diffusiophoresis in addition to the other scavenging mechanisms referred to above results. As mentioned earlier, though due to the water-soluble portion of particles, we cannot discuss about total range of particles, there is a good agreement between the raindrop size dependence of scavenging coefficient for particles and the number size distribution of particles with radius 1 μm scavenged by each size raindrop in Fig. 3.

3.2. Chemical properties

Table 1 summarizes statistical mass data for individual particles contained in the size-classified raindrops. The raindrop size dependence of every elemental mass showing the peak at $Rd_{0.7mm}$ was found. The masses of crustal components and chlorine are predominantly high regardless of raindrop size. Whereas, the several elements, which may be considered to the anthropogenic derived sources like vanadium, chromium, manganese, cobalt, nickel, copper, and zinc are detected as the minor elements. A comprehensive description of these minor elements will be presented in the end of this paper. The mass of Cl accounts for roughly 18%, 5%, 23%, 3%, and 9% of total elemental mass in the raindrop size $Rd_{<0.5mm}$, $Rd_{0.5mm}$, $Rd_{0.7mm}$, $Rd_{1.0mm}$, and $Rd_{>1.7mm}$, respectively. Whereas, the percentages calculated from the mass ratio of $\sum$ soil components/$\sum$ total element are 69%, 75%, 68%, 88%, and 81% at $Rd_{<0.5mm}$, $Rd_{0.5mm}$, $Rd_{0.7mm}$, $Rd_{1.0mm}$, and $Rd_{>1.7mm}$, respectively. The mass of Cl at $Rd_{0.7mm}$ (in the range of 2.8×10^{-3} pg to 1.0×10^{0} pg with average 2.9×10^{-1} pg) is higher, roughly 20 times more than those of other raindrop sizes. Wang and Guanghua (1996) reported that the high frequencies of chlorine measured in other areas of Japan during Asian dust storm events. It is suggested that the Asian dust storm particles were absorbed or coalesced with particles containing sea-salt during the long-range transport.

3.3. Particle classification by factor analysis

To classify the individual solid particles retained in size-resolved raindrops into several groups according to the elemental component, as one of the multivariate statistical techniques, factor analysis was applied. To carry out factor analysis, the 60 variables $\times 17$ cases matrixes of correlation coefficients for five-step raindrop

Table 1
Statistical summary of mass for 17 elements in individual Asian dust storm particles retained in size-segregated raindrops

	$Rd_{<0.5mm}$			$Rd_{0.5mm}$			$Rd_{0.7mm}$			$Rd_{1.0mm}$			$Rd_{>1.7mm}$		
	Min (pg)	Max (pg)	Mean (pg)	Min (pg)	Max (pg)	Mean (pg)	Min (pg)	Max (pg)	Mean (pg)	Min (pg)	Max (pg)	Mean (pg)	Min (pg)	Max (pg)	Mean (pg)
Al	2.8E−03	1.1E−01	1.2E−02	2.4E−03	2.3E−02	8.4E−03	5.9E−03	2.8E−01	7.3E−02	—	2.4E−01	1.1E−02	1.9E−03	1.3E−01	2.1E−02
Si	3.8E−03	1.0E−01	1.9E−02	6.4E−30	3.8E−02	2.2E−02	—	6.9E−01	1.0E−01	5.6E−03	4.4E−01	2.8E−02	3.1E−04	3.1E−01	4.4E−02
P	1.2E−0.3	6.2E−02	1.0E−02	2.2E−03	3.3E−02	1.2E−02	—	2.8E−01	5.7E−02	2.9E−03	1.4E−01	1.2E−02	2.77E−03	1.3E−01	1.8E−02
S	1.5E−03	8.0E−02	8.8E−03	9.3E−04	1.8E−01	1.4E−02	5.6E−04	1.8E−01	6.2E−02	—	2.0E−02	3.4E−03	9.8E−04	1.1E−01	9.6E−03
Cl	1.7E−03	8.2E−01	3.0E−02	4.8E−04	5.6E−02	5.6E−03	2.8E−03	1.0E+00	2.9E−01	—	1.5E−02	2.0E−03	4.7E−04	7.9E−01	2.1E−02
K	1.9E−03	1.1E+00	3.7E−02	6.9E−05	3.2E−02	4.5E−03	1.8E−02	8.5E−01	2.8E−01	—	5.9E−02	4.8E−03	6.8E−04	1.1E+00	4.3E−02
Ca	—	4.1E−01	3.0E−02	7.1E−04	4.1E−01	3.6E−02	1.8E−03	3.2E−01	6.5E−02	1.3E−04	6.8E−02	6.2E−03	5.2E−04	1.5E−01	1.3E−02
Sc	5.4E−05	3.6E−02	2.8E−03	3.1E−04	3.5E−02	3.4E−03	—	3.0E−02	8.4E−03	1.8E−04	6.8E−03	9.8E−04	1.1E−04	1.0E−02	1.7E−03
Ti	3.9E−05	8.4E−03	7.0E−04	—	4.5E−03	4.9E−04	4.3E−04	3.2E−01	1.5E−01	2.5E−04	4.0E−03	1.2E−03	1.9E−04	1.5E−01	5.5E−03
V	2.3E−06	4.3E−03	3.1E−04	—	7.9E−04	1.7E−04	1.6E−04	3.5E−02	1.7E−02	3.7E−05	1.7E−03	3.5E−04	3.2E−05	1.8E−02	1.2E−03
Cr	—	4.3E−03	4.4E−04	2.3E−04	9.7E−04	5.8E−04	2.2E−05	9.3E−03	2.7E−03	2.6E−04	2.1E−03	7.5E−04	3.5E−05	4.9E−03	8.4E−04
Mn	—	4.2E−03	3.3E−04	1.2E−04	8.0E−04	2.4E−04	1.7E−04	2.3E−02	3.8E−03	1.0E−04	5.1E−03	5.9E−04	7.5E−05	5.1E−03	1.0E−03
Fe	—	1.4E−01	7.1E−03	8.2E−04	4.3E−03	1.5E−03	1.0E−03	4.8E−02	1.3E−01	1.4E−03	1.1E−01	1.4E−02	6.7E−04	3.0E−01	3.6E−02
Co	—	1.2E−02	6.7E−04	7.7E−04	7.7E−04	2.2E−04	2.6E−04	3.2E−02	9.4E−03	1.5E−04	7.1E−03	1.1E−03	1.1E−04	2.0E−02	2.6E−03
Ni	5.7E−06	3.8E−03	2.5E−04	—	2.1E−03	1.4E−04	2.1E−04	1.7E−03	5.6E−04	9.7E−05	8.2E−04	2.1E−04	1.2E−04	1.5E−02	5.9E−04
Cu	2.1E−05	3.9E−03	1.4E−04	1.1E−04	1.7E−02	1.8E−03	1.2E−03	1.5E−02	2.5E−03	—	4.6E−03	8.9E−04	5.1E−05	3.3E−02	2.0E−03
Zn	8.0E−05	1.8E−01	8.1E−03	3.6E−06	1.8E−02	8.9E−04	6.9E−04	2.5E−02	4.4E−03	—	5.7E−03	3.5E−04	1.1E−04	2.5E−02	1.7E−03

Rd means the mesh size.

sizes were constructed. The procedure of factor analysis as follows: Choosing the variables and cases (the number of variable and case)—Choosing the factoring method (extraction method and the number of factors)—Construction of the matrix of correlation coefficients—Factor rotating (Varimax with Kaiser normalization)—Estimation of the rotating result—Calculation of factor score. Components in our data set had the missing value of 1–3%. Since missing data pose problems for factor analysis, they were replaced by mean values. Table 2 summarizes the result of factor analysis showing the sources identified from 17-element in solid particles retained in size-segregated raindrops. Individual solid particles were successfully divided into four factors (94% cumulative), three factors (98% cumulative), two factors (85% cumulative), three factors (96% cumulative), and four factors (96% cumulative) in the raindrop size $Rd_{<0.5mm}$, $Rd_{0.5mm}$, $Rd_{0.7mm}$, $Rd_{1.0mm}$, and $Rd_{>1.7mm}$, respectively. As the first factor, particles with crustal > marine-rich, particles with crustal > sulfur > marine-rich and, particles with marine > crustal-rich, particles with crustal > sulfur-rich, and particles with crustal > sulfur-rich were classified in the raindrop size $Rd_{<0.5mm}$, $Rd_{0.5mm}$, $Rd_{0.7mm}$, $Rd_{1.0mm}$, and $Rd_{>1.7mm}$, respectively. In the second factor, only crustal-rich particles were grouped in every raindrop size except $Rd_{0.7mm}$. Though we cannot fully explain the chemical mixing state of individual solid particles remained in size-segregated raindrops from the interpretation of the factors, the second factor seems to indicate that the dust storm particles without the internal mixing with marine and other artificial particles were scavenged by each raindrop size at our sampling site. In addition, the crustal component identified in the second factor suggests that sea-salt and water-soluble anthropogenic components like sulfur mixed with dust storm particles in the air were probably ionized in raindrops. The third factor seems to express the modification of Asian dust storm particles by the mixing processes with sea-salt and sulfur.

3.4. Elemental hygroscopicity of particles

As already pointed out, for the interpretation of the number size distribution of particles scavenged by raindrop, one of the difficulties is that we do not know the hygroscopic portion of Asian dust storm particles. This water-soluble fraction of an aerosol determines its chemical and physical properties and also its behavior. The origin of the aerosol and its atmospheric transport influence its solubility. To estimate the hygroscopic portion for S, Cl, K, and Ca in individual particles retained in size-segregated raindrop, the ratios of these components to Al were plotted in Fig. 5. Also those in atmospheric particles collected in Asian dust storm events by Ma et al. (2004) were compared. By comparing

Table 2
Sources identified each factor derived from 17-element in insoluble particles retained by size-segregated raindrops

	Factor 1		Factor 2		Factor 3		Factor 4		
Raindrop size	Identification	% of variance	Identification	% of variance	Identification	% of variance	Identification	% of variance	Cumulative %
$Rd_{<0.5mm}$[a]	Crustal > Marine	48.49	Crustal	28.32	Crustal > Marine > Sulfur	1.064	Artificial > Crustal[b]	6.79	94.24
$Rd_{0.5mm}$	Crustal > Sulfur > Marine	61.37	Crustal	28.45	Sulfur > Marine > Crustal	7.63	—	—	97.24
$Rd_{0.7mm}$	Marin > Crustal[c]	52.92	Crustal > Marine[d]	32.38	—	—	—	—	85.20
$Rd_{1.0mm}$	Crustal > Sulfur	63.48	Crustal	17.84	Crustal > Sulfur > Marine	14.97	—	—	96.30
$Rd_{<1.7mm}$	Crustal > Sulfur	46.06	Crustal[e]	32.80	Crustal > Sulfur > Marine	9.94	Crustal[f]	6.86	95.66

[a] Mesh size.
[b] Zn-rich.
[c] K-rich.
[d] Ti-rich.
[e] Fe-rich.
[f] Si-rich.

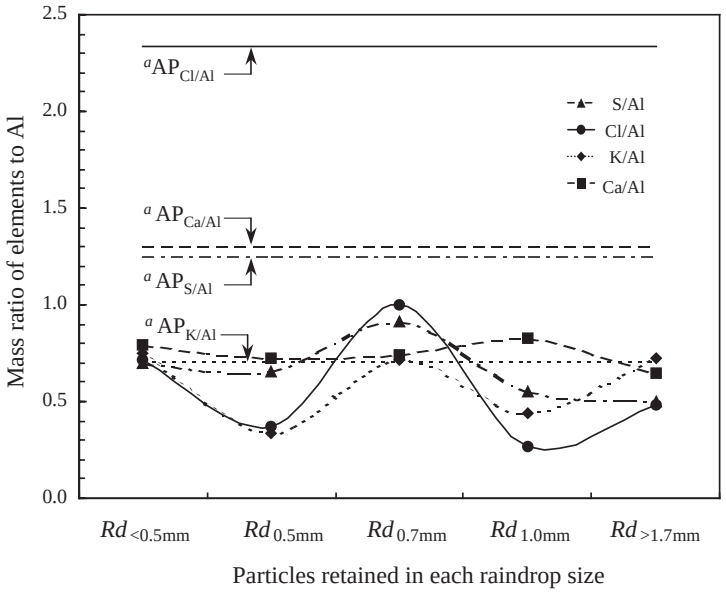

Fig. 5. Mass ratios of elements to Al in individual solid particles retained in size-segregated raindrops. *Rd* and *a* are mean raindrop diameter and atmospheric particles (Ma et al., 2004), respectively.

the ratios of representative water-soluble components to Al in raindrop-retained particles and the ambient dust particles, the elemental hygroscopicity of particles can be indirectly assumed. The average ratios of S/Al, Cl/Al, K/Al, and Ca/Al in 255 Asian dust storm particles were 1.15, 2.34, 0.71, and 1.30, respectively. As shown in Fig. 5, the average ratios in particles scavenged in raindrops were found to be raindrop size dependent showing relatively or significantly low levels compared to those in atmospheric Asian dust storm particles. Especially Cl/Al ratios of particles scavenged by each raindrop size show significantly low level through every raindrop size. This result indicates that Cl in solid particles retained in raindrop has large water-soluble portion. More than 80% of Cl mass in particles retained in raindrops with $Rd_{0.5mm}$ and $Rd_{1.0mm}$ are occupied by water-soluble fraction. While on the other hand, K shows the relatively slight water-soluble portion. Water-soluble portion of Ca was found to be relatively constant with 36–50%. Whereas, that of Cl shows the violent raindrop size dependence. The particles in raindrops larger than 1.0 mm diameter contained large portion of water-soluble S ($>56\%$).

To study the hygroscopic property of individual Asian dust storm particles, Okada et al. (1990) observed the morphology of the Asian dust storm particles collected at Nagasaki, Japan before and after dialysis with water. By change in the features of the particles before and after dialysis, they reported the presence of water-soluble fraction around the particles. Especially S and Ca are largely removed from the original Asian dust storm particles. In the study of the factors influencing aerosol solubility during cloud processes, Desboeufs et al. (2001) conducted the leaching experiments on the both original aerosols of Sahara loess and anthropogenic aerosols at pH 4.7. In their report for the solubility % of all elements after 120 min leaching, for all the elements, the solubility is higher in the fly ash than the loess particles. Also several other studies have already emphasized that the crustal aerosols are less soluble than marine or anthropogenic aerosols (Jickells et al., 1992; Spokes et al., 1994; Spokes and Jickells, 1996).

3.5. Chemical mixing state of individual particles and residues in raindrop

Fig. 6 draws the example XRF images of Fe, Si, Cl, and Ca in individual solid particles retained in large raindrop with $Rd_{>1.7mm}$. These visualized elemental maps for Fe, Si, Cl, and Ca enable us not only to presume the chemical mixing state of raindrop residual particles, but also to estimate their source profiles. For example, particles ♯19, ♯52, and ♯53 (in Fe map) indicate the chemical mixing state with soil derived components and Cl. Whereas, particle ♯1 drawn at abscissa 36: ordinate 10 in Fe map consists of only crustal components. Especially particle ♯0 (abscissa 10: ordinate 5) is composed of Fe. Consequently, from these four kinds of XRF images replayed corresponding to individual residual particles in raindrops, we can simply fractionate the visualized particle images into several groups.

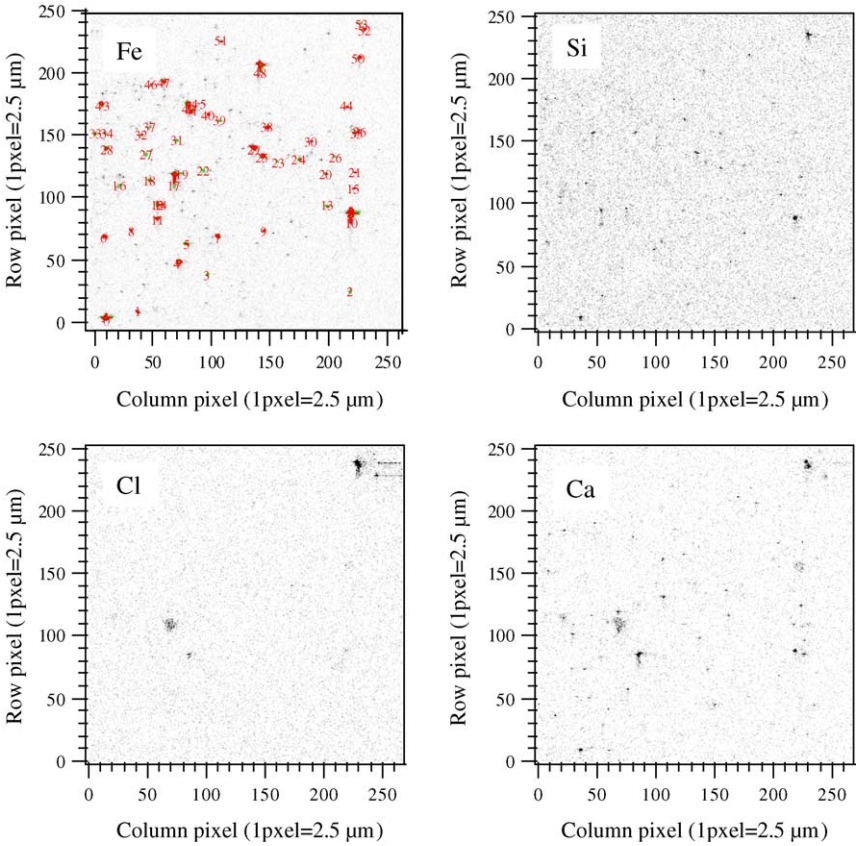

Fig. 6. XRF images of Fe, Si, Cl, and Ca in individual solid particles retained in Rd > 1.7 mm.

As mentioned earlier, it is possible to maintain residual materials on raindrop replica formed on collodion film. These retained matters could be the targets of micro-PIXE analysis. An example of elemental maps shown in Fig. 7 was drawn on a $27\,\mu m \times 27\,\mu m$ scanning area including several solid particles. Row and column are pixels corresponding beam scan area and the scale bar shows the intensity of characteristics X-ray count. Each elemental map could be drawn on the 128×128 pixels by scanning of about 1 μm micro beam on the sample surface. Several elements in and/or on residual matters were successfully detected by 2.6 MeV H^+ micro beam. Soil components such as Fe and K are distributed around row pixel ♯50: column pixel ♯50. Also, the small fraction of Cl and the large fraction of S are distributed at the same portion. The chemical mixing state with crustal and Cl in a portion of raindrop residue is in agreement with the results of individual solid particles retained in raindrop.

On the ground of these elemental maps drawn from XRF microanalysis and the results of factor analysis, the chemical mixing state of individual solid particles in size-classified raindrops was determined. Fig. 8 shows the occupation rate of each type of mixed particles retained in each size of raindrop. The percentage values were calculated from the fraction of each mixed particle number to the total particle number as a function of raindrop size. This result indicates that the chemical mixing states in solid particles are showing the strong raindrop size dependence. Though large portions of sea-salt and sulfur were probably dissociated, three types particles (mixed with crustal, sea-salt, and sulfur; mixed with crustal and sea-salt; mixed with crustal and sulfur) were found to be the dominant types in overall raindrop size. The mixed particles with crustal and sea-salt accounted for 48% and 85% of particles retained in small raindrops with $Rd_{<0.5mm}$ and $Rd_{0.7mm}$, respectively, whereas in the case of large raindrops ($Rd_{>1.0mm}$), the mixed particles with crustal and sulfur contributed to large portion. About the origin of this sulfur content, two possibilities can be presumed. As one of sulfur sources, $CaSO_4$ in desert soil can be considered. The other is the incorporation of anthropogenic sulfur into the Asian dust storm particles at the industrial areas in China and at the receptor area in Japan. According to the previous study (Ma et al., 2004), about 21% of $CaCO_3$ in Asian dust storm particles would be converted to $CaSO_4$ through the chemical reaction between $CaCO_3$

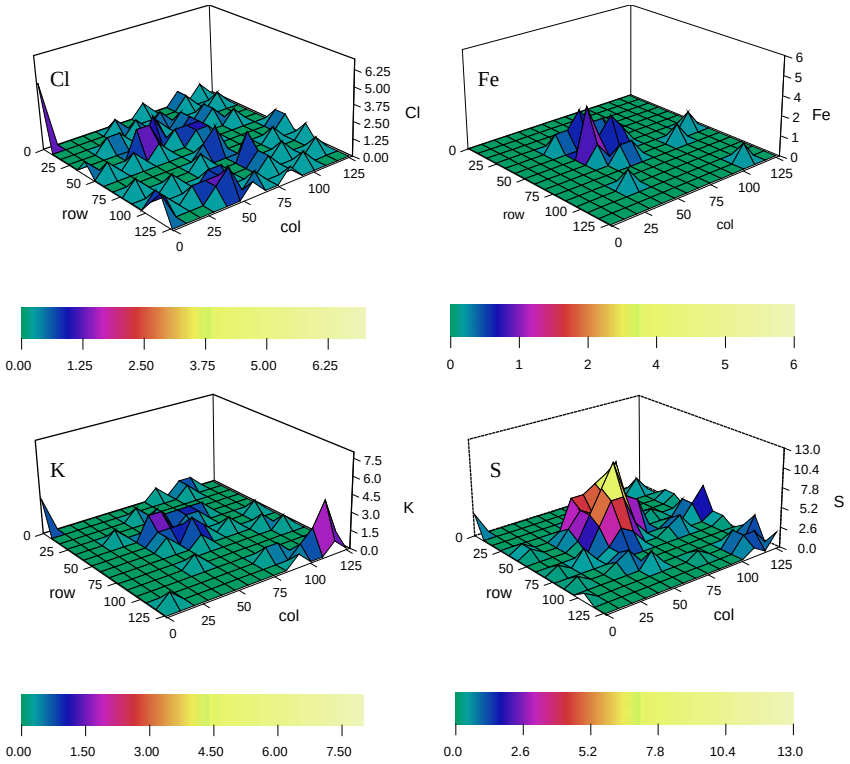

Fig. 7. An example of micro-PIXE elemental maps taken on a portion of single raindrop with 1.5 mm diameter. Micro beam scanning area is $27 \times 27\,\mu m^2$.

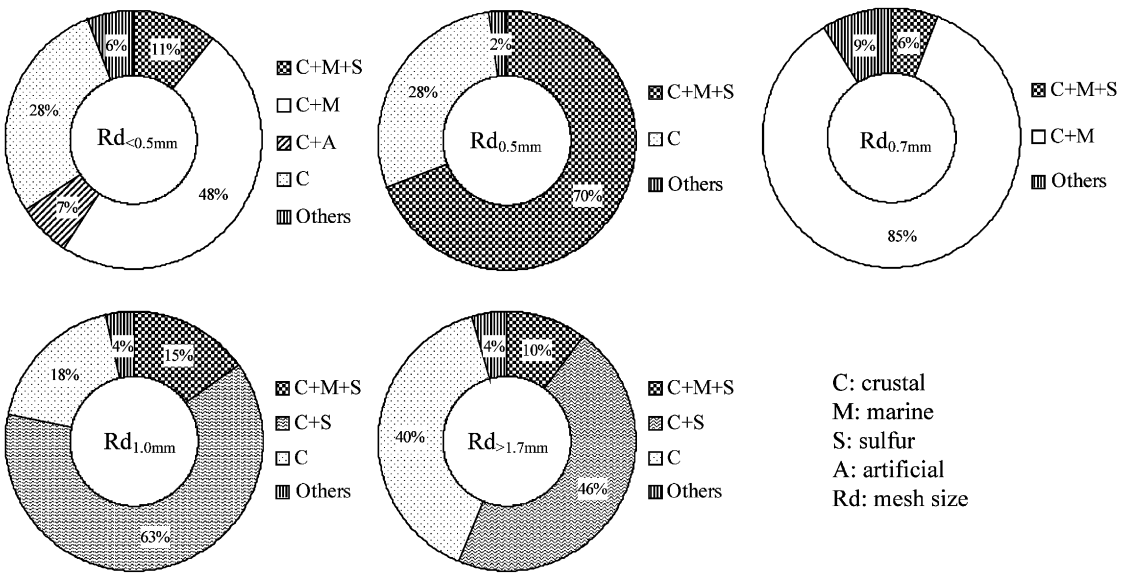

Fig. 8. Percentage of each mixed particles in the insoluble particles scavenged by each size of raindrop.

and H_2SO_4 during long-range transport. Elsewhere, as shown in Fig. 8, the particles derived from crust account for around 87%, 98%, 91%, 96%, and 96% of total particle number in the raindrop size with $Rd_{<0.5mm}$, $Rd_{0.5mm}$, $Rd_{0.7mm}$, $Rd_{1.0mm}$, and $Rd_{>1.7mm}$, respectively. It is therefore suggested that cloud condensation

nucleation was mainly initiated from crustal components in our sampling periods. Also the below cloud scavenging of crustal particles might occur during rainfall from cloud base to ground. Though to understand the mixing processes of dust storm particles with sea-salt and sulfur, one has to fully understand that how dust storm particles age and how anthropogenic pollutants are incorporated into this dust and marine particles, as the several mechanisms for the internal mixture of Asian dust storm particles with sea salt, Brownian coagulation, impaction by differential sedimentation, and coalescence of cloud droplets containing minerals with those containing sea salt can be considered. However as stated by Andreae et al. (1986) and Friedlander (1977), Brownian coagulation and impaction by differential sedimentation cannot explain internal mixture in particles with diameter of 2–4 μm during long-range transport. Therefore, the internal mixture of Asian dust storm particles with sea salt in this sampling period was probably occurred by the cloud condensation nuclei in an atmosphere with low supersaturation. Cloud droplets should be formed individually on the Asian dust storm particles and sea salt particles in the marine boundary layer. Then the internal mixing of dust particles with marine particles should occur on evaporation of the cloud droplets. The fraction of different residual particle types obtained by this work can be compared to the results of individual particle analysis conducted by Bruynseels et al. (1988). They collected the ambient aerosols and rain water samples in the Southern Bight of the North Sea and analyzed single particles by Laser Microprobe Mass Analysis (MAMMA) and Electron Probe X-ray Microanalysis (EPXMA). According to their results, in the aerosols collected from an air mass traveled from the Atlantic Ocean along the coast of North France, pure sea salt constituted the most abundant particle type, while aluminosilicates amounted to about 20% and mixed seasalt/aluminosilicate, carbonaceous particles, $CaSO_4$ and spherical iron oxides contributed each 5–10%. In rainwater, about 40% of the particles appeared to be aluminosilicates from fly ash and dust dispersal, but more than 50% consisted of SiO_2.

To distinguish between desert soil-originated and human activity source for the minor elements, interelement ratios are compared in conjunction with raindrop size. Fig. 9 shows the ratio of each elemental mass to Al mass for individual particles retained in size-segregated raindrops. Since the levels of Mn/Al ratios are around those in desert soil (Ma, 2001), a plot of Mn/Al ratios versus raindrop size indicates that the particles contained in relatively smaller raindrops ($Rd_{<1.0mm}$) were probably derived form desert soil. On the other hand, Mn/Al ratios of particles in large raindrops ($Rd_{>1.0mm}$) show high values indicating anthropogenic sources such as oil burning. The mass ratio for other trace elements were found to be overwhelmingly higher levels with noticeable fluctuation among raindrop sizes than those in soil through whole range of raindrop size. As a consequence, this result suggested that minor trace elements in particles scavenged raindrops were attributed to human activities like oil burning, iron industry, automobile driving and so on. Coal combustion is one of the other sources of Al. When Al originated from coal combustion is present in the atmosphere, the ratio of trace element to Al will be underestimated. Since coal combustion is a major source of air pollution in China, if air parcel was contaminated in industrial area of China during transport, we cannot exclude the possibility of this underestimation of interelement ratios.

4. Summary

To study the nature of individual solid particles retained in raindrops fallen during Asian dust storm event, the size-classified raindrops were collected and analyzed. For the analysis of elemental components in individual solid particles, XRF microprobe system was applied. Moreover, the physical properties of particles in each size raindrops were compared to the calculated particle-scavenging coefficient. Particles with radius around 0.5 μm show the maximum number size distribution at raindrops collected on mesh with pore size 0.5 mm. One the other hand, the number size distribution for particles with radius 1 μm was decreased with increasing raindrop size. There was a good agreement between the calculated raindrop size dependence of scavenging coefficient for particles and the measured number size distribution of particles with radius 1 μm. Elemental mass of solid particles retained in raindrop showed the strong raindrop size dependence with the peak at $Rd_{0.7mm}$. The masses of crustal components and chlorine were predominantly high regardless of raindrop size. Individual solid particles were successfully divided into several factors as a function of raindrop size. To estimate the hygroscopic portion for S, Cl, K, and Ca in individual particles retained in size-segregated raindrop, the ratios of these components to Al were compared to those in atmospheric particles collected in Asian dust storm events. According to the elemental maps and the results of factor analysis, the chemical mixing state of individual solid particles in size-classified raindrops was determined. In the case of large raindrops the mixed particles with crustal and sulfur contributed to large portion of particle number, while the mixed particles with crustal and sea-salt accounted for large fraction of particle population retained in small raindrops, By comparing the interelemental ratios in solid particles retained in each size raindrops to those in desert soil, it is suggested that the minor trace elements in particles scavenged raindrops were attributed to human activities

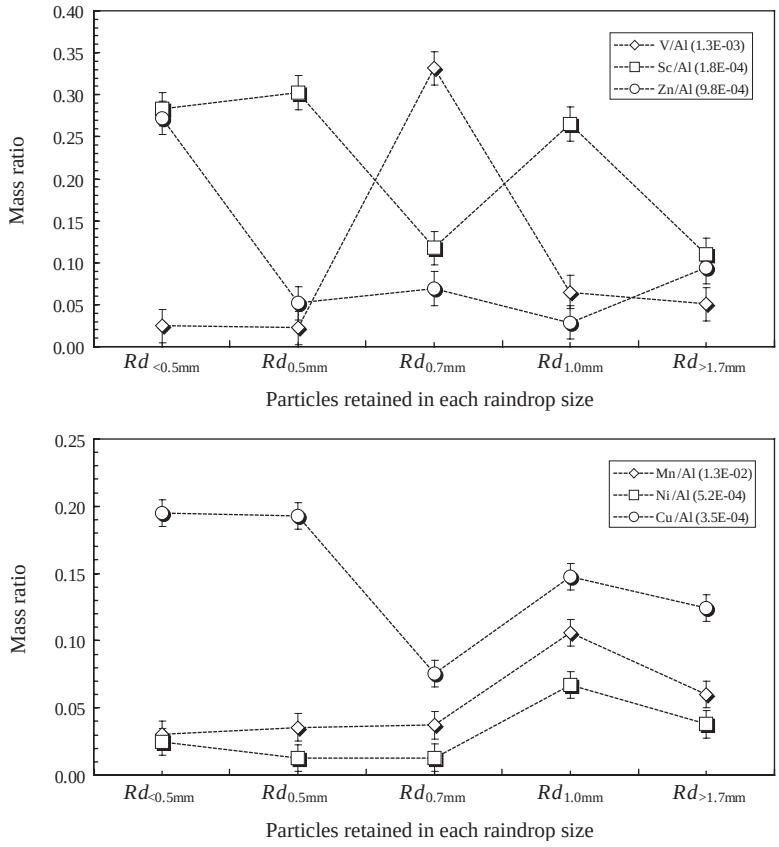

Fig. 9. The ratio of each minor elemental mass to Al mass for individual particles retained in size-segregated raindrops. R_d means the mesh size of size-segregated raindrop collector. The numbers in parenthesis in index boxes are the ratio of each element to Al in four-desert soil (Ma, 2001).

like oil burning, iron industry, and automobile driving. Though the in-cloud scavenging and the precipitation removal of Asian dust storm particles from the atmosphere have been expected, our results obtained from a combination of single and size-resolved raindrop sampling methods and microbeam analytical technique newly make certain of the truth that the wet removal processes is one of final dissipation mechanisms of Asian dust storm particles absorbed or coalesced with particles containing marine and artificial components during the long-range transport.

Acknowledgements

This study was supported in part by funds from the Grant-in-Aid for Scientific Research on Priority Areas under Grant No. 14048212 and 14048213 from Ministry of Education, Culture, Sports, Science and Technology (MEXT), Japan. Also this study was partly carried out under the aid of the program "Establishment of COE on Sustainable-Energy System". The synchrotron radiation experiments were performed at the SPring-8 with approval of the Japan Synchrotron Radiation Research Institute (JASRI) (Proposal No. 2002B0395-NOS-np). Finally, the authors wish to express thanks to all the members of SPring-8, BL-37XU for their experimental support.

References

Andreae, M.O., Charlson, J.C., Bruynseels, F., Storms, H., Van Grieken, R., Maenhant, W., 1986. Internal mixture of sea salt, silicates and excess sulfate in marine aerosols. Science 232, 1620–1623.

Beard, K.V., 1976. Terminal velocity and shape of cloud and precipitation drops aloft. Journal of Atmospheric Science 33, 851–864.

Braaten, D.A., Cahill, T.A., 1986. Size and composition Asian dust transported to Hawaii. Atmospheric Environment 20, 1105–1109.

Bruynseels, F., Storms, H., Grieken, R.V., Auwera, L.V., 1988. Characterization of North Sea aerosols by individual particle analysis. Atmospheric Environment 22, 2593–2602.

Byrne, M.A., Jennings, S.G., 1993. Scavenging of submicrometer aerosol particles by water drops. Atmospheric Environment 27A, 2099–2105.

Chate, D.M., Kamra, A.K., 1997. Collection efficiencies of large water drops collection aerosol particles of various densities. Atmospheric Environment 31, 1631–1635.

Chen, W.H., 2002. An analysis of gas absorption by a liquid aerosol in a stationary environment. Atmospheric Environment 36, 3671–3683.

Chun, Y.S., Kim, J.Y., Choi, J.C., Boo, K.O., Oh, S.N., Lee, M.H., 2001. Characteristic number size distribution of aerosol during Asian dust period in Korea. Atmospheric Environment 35, 2715–2721.

Darzi, M.D., Winchester, W., 1982. Aerosol characteristics at Mauna Loa observatory, Hawaii, after East Asia dust storm episodes. Journal of Geophysical Research 87, 1251–1258.

Desboeufs, K.V., Losno, R., Colin, J.L., 2001. Factors influencing aerosol solubility during cloud processes. Atmospheric Environment 35, 3529–3537.

Duce, R.A., Unni, C.K., Ray, B.J., Prospere, J.M., Merrill, T., 1980. Long-range atmospheric transport of soil dust from Asia to the tropical north Pacific: temporal variability. Science 209, 1522–1524.

Flossmann, A.I., Hall, W.D., Purppacher, H.R., 1985. A theoretical study of the wet removal of atmospheric pollutants. Part I: the redistribution of aerosol particles captured through nucleation and impaction scavenging by growing cloud drops. Journal of the Atmospheric Sciences 42, 583–606.

Friedlander, S.L., 1977. Smoke, Dust and Haze: Fundamentals of Aerosol Behavior. Wiley, New York, p. 317.

Greenfield, S.M., 1957. Rain scavenging of radioactive particulate matter from the atmosphere. Journal of Meteorology 14, 115.

Hayakawa, S., 2000. X-ray fluorescence method for trace analysis and imaging. Journal of Japanese Society for Synchrotron Radiation Research 13, 313–318 (in Japanese).

Hayakawa, S., Ikuta, N., Suzuki, M., Wakatsuki, M., Hirokawa, T., 2001. Generation of an X-ray microbeam for spectromicroscopy at SPring-8 BL39XU. Journal of Synchrotron Radiation 8, 328–330.

Ishii, Y., Tanaka, R., Isoya, A., 1996. Low-energy ion source characteristics for producing an ultra-fine microbeam. Nuclear Instruments and Methods in Physics Research B 113, 75–77.

Iwasaka, Y., Yamamoto, M., Imasu, R., Ono, A., 1988. Transport of Asian dust (KOSA) particles: importance of weak KOSA events on the geochemical cycle of soil particles. Tellus 40B, 494–503.

Jickells, T.D., Davies, T.D., Tranter, M., Landsberger, S., Jarvis, K., Abrahams, P., 1992. Trace elements in snow samples from the Scottish highlands: sources and dissolved/particulate distributions. Atmospheric Environment 26A, 393–401.

Lei, H.C., Tanner, P.A., 1997. The acidification process under the cloud in southwest China: observation results and simulation. Atmospheric Environment 31, 851–861.

Ma, C.J., 2001. New approaches for characterization of atmospheric particles and acid precipitation. Ph. D. dissertation, Kyoto University.

Ma, C.J., Kasahara, M., Höller, R., Kamiya, T., 2001a. Characteristics of single particles sampled in Japan during the Asian dust-storm period. Atmospheric Environment 35, 2707–2714.

Ma, C.J., Kasahara, M., Tohno, S., Kamiya, T., 2001b. A new approach for characterization of single raindrops. Water, Air and Soil Pollution 130, 1601–1606.

Ma, C.J., Kasahara, M., Tohno, S., Sakai, T., 2003. A replication technique for the collection of individual fog droplets and their chemical analysis using micro-PIXE. Atmospheric Environment 37, 4679–4686.

Ma, C.J., Kasahara, M., Tohno, S., Hayakawa, S., 2004. Properties of individual Asian dust storm particles collected at Kosan, Korea during ACE-Asia. Atmospheric Environment 38, 1133–1143.

Mashall, J.S., Palmer, M.W.M., 1948. The distribution of raindrop with size. Journal of Meteorology 5, 165–166.

McGann, K., Haag, I., Roder, A., 1993. The efficiency with drizzle and precipitation sized drops collide with aerosol particles. Atmospheric Environment 25A, 791–799.

Nicholson, K.W., Branson, J.R., Giess, P., 1991. Field measurements of the bellow-cloud scavenging of particulate material. Atmospheric Environment 25A, 771–777.

Okada, K., Naruse, H., Tanaka, T., Nemoto, O., Iwasaka, Y., Wu, P.M., Ono, A., Duce, R.A., Uematsu, M., Merrill, T., 1990. X-ray spectrometry of individual Asian dust-storm particles over the Japanese Island and the North Pacific Ocean. Atmospheric Environment 24A, 1369–1378.

Pilat, M.M., Prem, A., 1976. Calculated particle collection efficiencies of single droplets including inertial impaction, Brownian diffusion, diffusiophoresis and thermophoresis. Atmospheric Environment 10, 13–19.

Seinfeld, J.H., 1986. Atmospheric Chemistry and Physics of Air Pollution. Wiley-Interscience, New York, pp. 622–705.

Seinfeld, J.H., Pandis, S.N., 1998. Atmospheric Chemistry and Physics. Wiley, New York, pp. 1003–1013.

Slinn, W.G.N., 1984. Precipitation scavenging, atmospheric science and power production. In: Randerson, D. (Ed.), National Technical Information Service, US Deptartment of Commerce. Springfield, VA, USA, pp. 466.

Slinn, W.G.N., Hales, J.M., 1971. A revaluation of the role of thermophoresis as a mechanism of in and below cloud scavenging. Journal of Atmospheric Science 28, 1465.

Spokes, J.J., Jickells, T.D., 1996. Factors controlling the solubility of aerosol trace metals in the atmosphere and on mixing into seawater. Aquatic Geochemistry 1, 355–374.

Spokes, L.J., Jickells, T.D., Lim, B., 1994. Solubilisation of aerosol trace metals by cloud processing: a laboratory study. Geochimica and Cosmochimica Acta 58, 3281–3287.

Strauss, W., 1975. Industrial Gas Cleaning. Pergamon Press, New York, pp. 293–3005.

Tenberken, B., Bächmann, K., 1996. Analysis of individual raindrops by capillary zone electrophoresis. Journal of Chromatography A 755, 121–126.

Wang, X., Guanghua, Z., 1996. Some characteristics of the aerosol in Beijing. International Journal of PIXE 6, 361–365.